

A PATHWAY-BASED MEAN-FIELD MODEL FOR *E. COLI* CHEMOTAXIS: MATHEMATICAL DERIVATION AND KELLER-SEGEL LIMIT

GUANGWEI SI, MIN TANG, AND XU YANG

ABSTRACT. A pathway-based mean-field theory (PBMFT) was recently proposed for *E. coli* chemotaxis in [G. Si, T. Wu, Q. Quyang and Y. Tu, *Phys. Rev. Lett.*, 109 (2012), 048101]. In this paper, we derived a new moment system of PBMFT by using the moment closure technique in kinetic theory under the assumption that the methylation level is locally concentrated. The new system is hyperbolic with linear convection terms. Under certain assumptions, the new system can recover the original model. Especially the assumption on the methylation difference made there can be understood explicitly in this new moment system. We obtain the Keller-Segel limit by taking into account the different physical time scales of tumbling, adaptation and the experimental observations. We also present numerical evidence to show the quantitative agreement of the moment system with the individual based *E. coli* chemotaxis simulator.

1. INTRODUCTION

The locomotion of *Escherichia coli* (*E. coli*) presents a tumble-and-run pattern ([4]), which can be viewed as a biased random walk process. In the presence of chemoeffector with nonzero gradients, the suppression of direction change (tumble) leads to chemotaxis toward the high concentration of chemoattractants ([1, 5]). Great efforts have been put into understanding the chemotactic sensory system of *E. coli* ([15, 30, 32]). The chemotaxis signaling pathway belongs to the class of two-component sensory system, which consists of sensors and response regulators. The chemotaxis sensor complex is composed of transmembrane chemo-receptors, the adaptor protein CheW, and the histidine kinase CheA. The response regulator CheY controls the tumbling frequency of the flagellar motor ([16]). Adaptation is carried out by the two enzymes, CheR and CheB, which control the kinase

Date: April 29, 2013.

G.S. was partially supported by NSF of China under Grants No. 11074009 and No. 10721463 and the MOST of China under Grants No. 2009CB918500 and No. 2012AA02A702. M.T. was partially supported by Shanghai Natural Science Foundation of Shanghai under Grant No. 12ZR1445400. X.Y. was partially supported by the startup funding of Department of Mathematics, University of California, Santa Barbara. G.S. would like to thank Yuhai Tu for valuable discussions and Tailin Wu for his early work on simulation.

activity by modulating the methylation level of receptors ([32]). Because of slow adaptation process, receptor methylation level serves as the memory of cells, and cells decide whether to run or tumble by comparing receptor methylation level to local environments.

In the modeling literature, bacterial chemotaxis has been described by the Keller-Segel (K-S) model at the population level ([20]), where the drift velocity is given by empirical functions of chemoeffector gradient. It has successfully explained the chemotaxis phenomenon in slowly changing environments ([29]), however fails to make good predictions in rapidly changing ones ([34]) and the volcano effects ([9, 26]). Besides that, the K-S model has also been mathematically proved to present nonphysical blowups in high dimension when initial total mass reaches the critical level ([6–8]). In order to understand bacterial behavior from the individual dynamics, kinetic models have been also developed by considering the velocity-jump process ([3, 17, 28]), and the K-S model can be systematically derived by taking the hydrodynamic limit of kinetic models (*e.g.* [10, 14]). All the above mentioned models are phenomenological and do not take into account the signaling transduction and adaptation process.

Nowadays, modern experimental technologies have been able to quantitatively measure the dynamics of signaling pathways of *E. coli* ([2, 11, 24, 27]), which has led to successful modeling of the pathway dynamics ([21, 23, 31]). These works make possible the verification of predictive agent-based models that include the intracellular signaling pathway dynamics. It is of great biological interest to understand the molecular origins of chemotaxis behavior of *E. coli* by deriving population-level model based on the underlying signaling pathway dynamics ([12, 25]). Particularly in [25], the authors developed a pathway-based mean field theory (PBMFT) that incorporated the most recent quantitatively measured signaling pathway, and explained a counter-intuitive experimental observation which showed that in a spatial-temporal fast-varying environment, there exists a phase shift between the dynamics of ligand concentration and center of mass of the cells [34]. Especially, when the oscillating frequency is comparable to the adaptation rate of *E. coli*, the phase shift becomes significant. Apparently this is a phenomenon that can not be explained by the K-S model.

In this paper, we study PBMFT for *E. coli* chemotaxis from a mathematical point of view. Specifically we derive a new moment system of PBMFT using the moment closure technique in kinetic theory. The new system is hyperbolic with linear convection terms. Under certain assumptions, the derived moment system gets to the original model in [25], and especially the assumption on the methylation difference made in [25] can be understood explicitly in this new system. Taking into account the different physical time scales of the tumbling, adaptation and experimental observation, we connect the moment system to the K-S model

(in the parabolic scaling). The agreement of the moment system with the signaling pathway-based *E. coli* chemotaxis agent-based simulator (SPECS [19]) will be provided numerically in the environment of spatial-temporal varying ligand concentration.

The rest of the paper is organized as follows. We introduce the pathway-based kinetic model incorporating the intracellular adaptation dynamics in Section 2. In Section 3, assuming the methylation level is locally concentrated, we are able to build the moment system by using the moment closure technique in one dimension. Furthermore, the modeling assumption will be justified both analytically and numerically. Section 4 illustrates why K-S model is valid in the slow varying environments. We also give the connection of the moment system to the PBMFT model proposed in [25], and provide the quantitative agreement of the moment system with SPECS numerically. Two-dimensional moment system is derived in Section 5, and we make conclusive remarks in Section 6.

2. DESCRIPTION OF THE KINETIC MODEL

We shall start from the same kinetic model used in [25], which incorporates the most recent progresses on the chemo-sensory system ([24, 31]). The model is a one-dimensional two-flux model given by

$$(2.1) \quad \frac{\partial P^+}{\partial t} = -\frac{\partial(v_0 P^+)}{\partial x} - \frac{\partial(f(a)P^+)}{\partial m} - \frac{z(m)}{2}(P^+ - P^-),$$

$$(2.2) \quad \frac{\partial P^-}{\partial t} = \frac{\partial(v_0 P^-)}{\partial x} - \frac{\partial(f(a)P^-)}{\partial m} + \frac{z(m)}{2}(P^+ - P^-).$$

In this model, each single cell of *E. coli* moves either in the “+” or “−” direction with a constant velocity v_0 . $P^\pm(t, x, m)$ is the probability density function for the cells moving in the “ \pm ” direction, at time t , position x and methylation level m .

The intracellular adaptation dynamics is described by

$$(2.3) \quad \frac{dm}{dt} = f(a) = k_R(1 - a/a_0),$$

where the receptor activity $a(m, [L])$ depends on the intracellular methylation level m as well as the extracellular chemoattractant concentration $[L]$, which is given by

$$(2.4) \quad a = (1 + \exp(NE))^{-1}.$$

According to the two-state model in [21, 23], the free energy is

$$(2.5) \quad E = -\alpha(m - m_0) + f_0([L]), \quad \text{with} \quad f_0([L]) = \ln\left(\frac{1 + [L]/K_I}{1 + [L]/K_A}\right).$$

In (2.3), k_R is the methylation rate, a_0 is the receptor preferred activity that satisfies $f(a_0) = 0$, $f'(a_0) < 0$. N , m_0 , K_I , K_A represent the number of tightly coupled receptors, basic methylation level, and dissociation constant for inactive receptors and active receptors respectively.

We take the tumbling rate function $z(m, [L])$ in [25],

$$(2.6) \quad z = z_0 + \tau^{-1}(a/a_0)^H,$$

where z_0 , H , τ represent the rotational diffusion, the Hill coefficient of flagellar motor's response curve and the average run time respectively. We refer the readers to [25] and the references therein for the detailed physical meanings of these parameters.

More generally, the kinetic model incorporating chemo-sensory system is given as below,

$$(2.7) \quad \partial_t P = -\mathbf{v} \cdot \nabla_{\mathbf{x}} P - \partial_m(f(a)P) + Q(P, z),$$

where $P(t, \mathbf{x}, \mathbf{v}, m)$ is the probability density function of bacteria at time t , position \mathbf{x} , moving at velocity \mathbf{v} and methylation level m .

The tumbling term $Q(P, z)$ is

$$(2.8) \quad Q(P, z) = \oint_{\Omega} z(m, [L], \mathbf{v}, \mathbf{v}') P(t, \mathbf{x}, \mathbf{v}', m) d\mathbf{v}' - \oint_{\Omega} z(m, [L], \mathbf{v}', \mathbf{v}) d\mathbf{v}' P(t, \mathbf{x}, \mathbf{v}, m),$$

where Ω represents the velocity space and the integral

$$\oint = \frac{1}{|\Omega|} \int_{\Omega}, \quad \text{where } |\Omega| = \int_{\Omega} d\mathbf{v},$$

denotes the average over Ω . $z(m, [L], \mathbf{v}, \mathbf{v}')$ is the tumbling frequency from \mathbf{v}' to \mathbf{v} , which is also related to the activity a as in (2.6). The first term on right-hand side of (2.8) is a gain term, and the second is a loss term.

3. ONE-DIMENSIONAL MEAN-FIELD MODEL

In this section, we derive a new moment system of PBMFT from (2.1)-(2.2) based on the assumption that the methylation level is locally concentrated. This assumption will be justified by the numerical simulations using SPECS and the formal analysis in the limit of $k_R \rightarrow \infty$. To simplify notations, we denote $\int_0^{+\infty}$ by \int in the rest of this paper.

3.1. Derivation of a new moment system of PBMFT. Firstly, we define the macroscopic quantities, density, density flux, momentum (on m) and momentum flux as follows,

$$(3.1) \quad \rho(x, t) = \int (P^+ + P^-) dm, \quad J_{\rho}(x, t) = \int v_0(P^+ - P^-) dm;$$

$$(3.2) \quad q(x, t) = \int m(P^+ + P^-) dm, \quad J_q(x, t) = \int v_0 m(P^+ - P^-) dm.$$

The average methylation level $M(t, x)$ is defined as

$$(3.3) \quad M = \frac{q}{\rho}.$$

For simplicity, we also introduce the following notations

$$(3.4) \quad \begin{aligned} Z &= z(M(t, x)), & \frac{\partial Z}{\partial m} &= \frac{\partial z}{\partial m} \Big|_{m=M}, \\ F &= f(a(M(t, x))), & \frac{\partial F}{\partial m} &= \frac{\partial f}{\partial m} \Big|_{m=M}. \end{aligned}$$

Assumption A. We need the following condition to close the moment system,

$$\frac{\int (m - M)^2 P^\pm dm}{\int P^\pm dm} \ll 1.$$

Remark. Physically this assumption means, the distribution functions P^\pm is localized in m , and the variation of averaged methylation is small in both moving directions “ \pm ”.

Integrating (2.1)+(2.2) with respect to m yields the equation for density

$$\frac{\partial \rho}{\partial t} + \frac{\partial J_\rho}{\partial x} = 0.$$

Integrating $v_0 \times (2.1) - v_0 \times (2.2)$ with respect to m produces

$$\begin{aligned} \frac{\partial J_\rho}{\partial t} &= -v_0^2 \frac{\partial \rho}{\partial x} - v_0 \int z(m)(P^+ - P^-) dm \\ &\approx -v_0^2 \frac{\partial \rho}{\partial x} - v_0 \int \left(z(M) + \frac{\partial z}{\partial m} \Big|_{m=M} (m - M) \right) (P^+ - P^-) dm \\ &= -v_0^2 \frac{\partial \rho}{\partial x} - Z J_\rho - \frac{\partial Z}{\partial m} (J_q - M J_\rho), \end{aligned}$$

where we have used Assumption A in the second step and the notations in (3.3), (3.4) in the third step.

Similarly, integrating $m \times (2.1) + m \times (2.2)$ with respect to m gives

$$\begin{aligned} \frac{\partial q}{\partial t} &= -\frac{\partial J_q}{\partial x} + \int f(a)(P^+ + P^-) dm \\ &\approx -\frac{\partial J_q}{\partial x} + \int \left(f(a)|_{m=M} + \frac{\partial f}{\partial m} \Big|_{m=M} (m - M) \right) (P^+ + P^-) dm \\ &= -\frac{\partial J_q}{\partial x} + F \rho + \frac{\partial F}{\partial m} (q - M \rho) \\ &= -\frac{\partial J_q}{\partial x} + F \rho, \end{aligned}$$

where we have used an integration by parts in the first step and the definition of M in (3.3) in the last step.

Integrating $v_0 m \times (2.1) - v_0 m \times (2.2)$ with respect to m yields

$$\begin{aligned}
\frac{\partial J_q}{\partial t} &= -v_0^2 \frac{\partial q}{\partial x} + v_0 \int f(a)(P^+ - P^-) dm - v_0 \int z(m)m(P^+ - P^-) dm \\
&\approx -v_0^2 \frac{\partial q}{\partial x} + v_0 \int \left(f(a)|_{m=M} + \frac{\partial f}{\partial m} \Big|_{m=M} (m - M) \right) (P^+ - P^-) dm \\
&\quad - v_0 \int \left((z(m)m)|_{m=M} + \frac{\partial(z(m)m)}{\partial m} \Big|_{m=M} (m - M) \right) (P^+ - P^-) dm \\
&= -v_0^2 \frac{\partial q}{\partial x} + FJ_\rho + \frac{\partial F}{\partial m} (J_q - MJ_\rho) - ZMJ_\rho - \left(\frac{\partial Z}{\partial m} M + Z \right) (J_q - MJ_\rho) \\
&= -v_0^2 \frac{\partial q}{\partial x} + FJ_\rho + \frac{\partial F}{\partial m} (J_q - MJ_\rho) - ZJ_q - \frac{\partial Z}{\partial m} M (J_q - MJ_\rho),
\end{aligned}$$

where we have used Assumption A in the last step.

Altogether, we obtain a closed moment system for ρ , J_ρ , q and J_q

$$(3.5) \quad \frac{\partial \rho}{\partial t} = -\frac{\partial J_\rho}{\partial x},$$

$$(3.6) \quad \frac{\partial J_\rho}{\partial t} = -v_0^2 \frac{\partial \rho}{\partial x} - ZJ_\rho - \frac{\partial Z}{\partial m} (J_q - MJ_\rho),$$

$$(3.7) \quad \frac{\partial q}{\partial t} = -\frac{\partial J_q}{\partial x} + F\rho,$$

$$(3.8) \quad \frac{\partial J_q}{\partial t} = -v_0^2 \frac{\partial q}{\partial x} + FJ_\rho + \frac{\partial F}{\partial m} (J_q - MJ_\rho) - ZJ_q - \frac{\partial Z}{\partial m} M (J_q - MJ_\rho).$$

Remark. The Taylor expansion in m gives a systematical way of constructing high order moment systems. Please see the Appendix for the derivation of second-order moment system.

3.2. Numerical Justification of Assumption A by SPECS. To justify the Assumption A, we simulate the distribution of m with SPECS in an exponential gradient ligand environment $[L] = [L]_0 \exp(Gx)$. SPECS is a well developed agent-based *E. coli* simulator that incorporates the physically measured signaling pathways and parameters. We refer the readers to [19] for its detailed description. In the simulation, cells exiting at one side of the boundary will enter from the other side, and the methylation level is reset randomly following the local distribution of m at the boundaries. Under this boundary condition, the system will reach the steady state after a period of transient process. The steady state distributions are shown in Figure 1. In each of the subfigures, the horizontal and vertical axes represent the position and the methylation level respectively. As shown in Figure 1, the distribution of methylation level is localized, and becomes wider when G increases. $M^\pm = \int m P^\pm dm$ are the average methylation levels for the right and left moving cells. One can also observe that $M^+ < M^-$ in the exponential increasing ligand concentration environment. This can be understood intuitively by noticing that the up gradient cells with lower methylation level come from left while the down gradient cells with higher methylation level come from right.

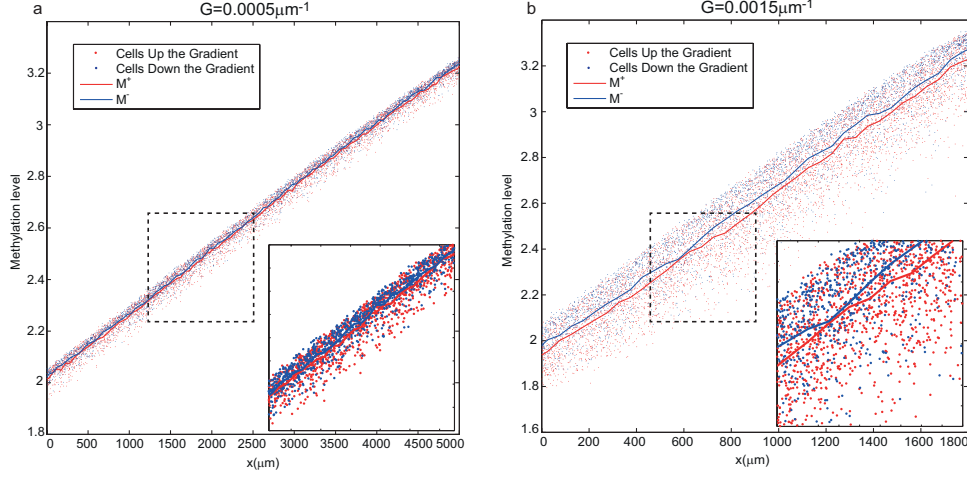


FIGURE 1. The distribution of cells' receptor methylation level for $G = 0.0005 \mu\text{m}^{-1}$ (a) and $G = 0.0015 \mu\text{m}^{-1}$ (b). The red dots represent cells moving to right while the blue ones represent those moving to left. M^\pm are the average methylation levels for the right and left moving cells respectively. In the simulation, we take $[L]_0 = 5K_I$. Other parameters used in the SPECS are the same as those proposed in [19].

In the exponential environment, the numerical variations of m are almost uniform in x . The maximum of the methylation level variation in the simulation domain is defined by

$$\sigma \equiv \max \sqrt{\frac{\int (m - M(x))^2 (P^+ + P^-) dm}{\int (P^+ + P^-) dm}}.$$

Assumption A is equivalent to the condition $\sigma \ll 1$. As shown in Figure 2, σ increases in G and decreases in k_R , but it is always small in the parameter regime we are interested in, *i.e.* Assumption A holds in these cases.

3.3. The localization of P^\pm in m in the limit of $k_R \gg 1$. We show by formal analysis that the assumption $\int (m - M)^2 P^\pm dm \ll 1$ is true when the adaptation rate $k_R \gg 1$. Denote

$$(3.9) \quad k_R = 1/\eta, \quad f(a) = f_\eta(a)/\eta,$$

then (2.1)-(2.2) become

$$(3.10) \quad \frac{\partial P^+}{\partial t} = -\frac{\partial(v_0 P^+)}{\partial x} - \frac{1}{\eta} \frac{\partial(f_\eta(a) P^+)}{\partial m} - \frac{z}{2}(P^+ - P^-),$$

$$(3.11) \quad \frac{\partial P^-}{\partial t} = \frac{\partial(v_0 P^-)}{\partial x} - \frac{1}{\eta} \frac{\partial(f_\eta(a) P^-)}{\partial m} + \frac{z}{2}(P^+ - P^-).$$

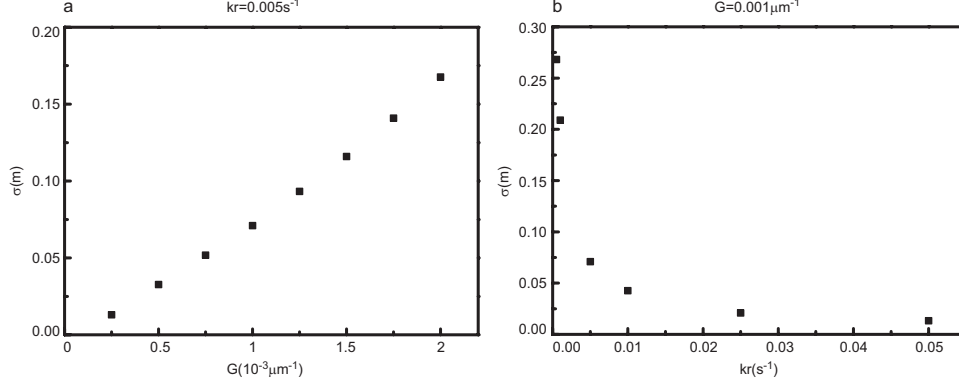


FIGURE 2. The maximum variances σ of m for different G and k_R . σ increases in G for a given k_R (a) and decreases in k_R with fixed G (b), but they are all small in the parameter regime we are interested in.

Integrating the above two equations with respect to m produces, for $P_R^\pm(t, x) = \int_0^R P^\pm(t, x, m) dm$ (R is an arbitrary positive constant),

$$(3.12) \quad \begin{aligned} \frac{\partial P_R^+}{\partial t} = & -\frac{\partial(v_0 P_R^+)}{\partial x} - \frac{1}{2} \int_0^R z(P^+ - P^-) dm \\ & - \frac{1}{\eta} f_\eta(a(R)) P^+(t, x, R) + \frac{1}{\eta} f_\eta(a(0)) P^+(t, x, 0), \end{aligned}$$

$$(3.13) \quad \begin{aligned} \frac{\partial P_R^-}{\partial t} = & \frac{\partial(v_0 P_R^-)}{\partial x} + \frac{1}{2} \int_0^R z(P^+ - P^-) dm \\ & - \frac{1}{\eta} f_\eta(a(R)) P^-(t, x, R) + \frac{1}{\eta} f_\eta(a(0)) P^-(t, x, 0). \end{aligned}$$

The probability density functions satisfy $P^\pm(t, x, m) \geq 0$, $\forall m \geq 0$, and thus $P_R^\pm(t, x)$ increases with R .

We consider the regime

$$(3.14) \quad \eta \ll 1, \quad \text{and} \quad f_\eta(a) \sim \mathcal{O}(1).$$

Then when $\eta \ll 1$, (3.12)-(3.13) indicate for $R \in (0, +\infty)$,

$$(3.15) \quad f_\eta(a(R)) P^\pm(t, x, R) = f_\eta(a(0)) P^\pm(t, x, 0) + \mathcal{O}(\eta).$$

We show by contradiction that when $\eta \rightarrow 0$, the boundary condition at $m = 0$ has to satisfy $f_\eta(a(0)) P^\pm(t, x, 0) \rightarrow 0$, $\forall (x, t) \in \mathbb{R} \times (0, +\infty)$. Otherwise, assume that

$$(3.16) \quad f_\eta(a(0)) P^\pm(t, x, 0) \rightarrow C(t, x) \neq 0, \quad \text{for some } (x, t) \in \mathbb{R} \times (0, +\infty).$$

Define

$$(3.17) \quad M_{a_0} = \frac{1}{\alpha} \left(-\frac{1}{N} \ln\left(\frac{1}{a_0} - 1\right) + \ln\left(\frac{1 + [L]/K_I}{1 + [L]/K_A}\right) \right) + m_0.$$

Then (2.3)-(2.4) imply

$$\begin{aligned} f_\eta(a(R)) &> 0, \quad \text{when } 0 < R < M_{a_0}; \\ f_\eta(a(R)) &< 0, \quad \text{when } R > M_{a_0}. \end{aligned}$$

Besides that, one has $P^\pm(t, x, R) > 0$, thus $f_\eta(a(R))P^\pm(t, x, R)$ will change sign for different R . On the other hand, when $\eta \ll 1$, (3.15), (3.16) imply that for $\forall R \in (0, +\infty)$, $f_\eta(a(R))P^\pm(t, x, R)$ has the same sign as $f_\eta(a(0))P^\pm(t, x, 0)$, which is a contradiction. Therefore, $f_\eta(a(0))P^\pm(t, x, 0) \rightarrow 0$, and as $\eta \rightarrow 0$,

$$(3.18) \quad f_\eta(a(R))P^\pm(t, x, R) \rightarrow 0, \quad \forall R \in (0, +\infty).$$

Then the definition of $f(a)$ in (2.3)-(2.4) gives that if $R \neq M_0$, $P^\pm(t, x, R) \rightarrow 0$, which implies when $\eta \rightarrow 0$,

$$(3.19) \quad P^\pm(x, t, m) = P_m^\pm \delta(m - M_0).$$

4. KELLER-SEGEL LIMIT AND CONNECTIONS TO THE ORIGINAL PBMFT

In this section, we derive the Keller-Segel limit from (3.5)-(3.8) by taking into account the different physical time scales of the tumbling, adaptation and experimental observations. We shall also connect the new moment system to the original PBMFT developed in [25]. Moreover, a numerical comparison of the moment system (3.5)-(3.8) with SPECS is provided in the environment of spatial-temporally varying concentration.

4.1. Keller-Segel limit by the parabolic scaling. We nondimensionalize the moment system (3.5)-(3.8) by letting

$$t = T\tilde{t}, \quad x = L\tilde{x}, \quad v_0 = s_0\tilde{v}_0,$$

where T, L are temporal and spatial scales of the system respectively. Then

$$J_\rho = s_0\tilde{J}_\rho, \quad J_q = s_0\tilde{J}_q,$$

and the system becomes (after dropping the “ \sim ”)

$$\begin{aligned} \frac{1}{T} \frac{\partial \rho}{\partial t} &= -\frac{s_0}{L} \frac{\partial J_\rho}{\partial x}, \\ \frac{s_0}{T} \frac{\partial J_\rho}{\partial t} &= -v_0^2 \frac{\partial \rho}{\partial x} \frac{s_0^2}{L} - \frac{s_0}{T_1} Z J_\rho - \frac{s_0}{T_1} \frac{\partial Z}{\partial m} (J_q - M J_\rho), \\ \frac{1}{T} \frac{\partial q}{\partial t} &= -\frac{s_0}{L} \frac{\partial J_q}{\partial x} + \frac{1}{T_2} F \rho, \\ \frac{s_0}{T} \frac{\partial J_q}{\partial t} &= -v_0^2 \frac{\partial q}{\partial x} \frac{s_0^2}{L} + F J_\rho \frac{s_0}{T_2} + \frac{\partial F}{\partial m} (J_q - M J_\rho) \frac{s_0}{T_2} - Z J_q \frac{s_0}{T_1} - \frac{\partial Z}{\partial m} M (J_q - M J_\rho) \frac{s_0}{T_1}, \end{aligned}$$

where T_1, T_2 are the average run and adaptation time scales respectively.

For *E. coli*, the average run time is at the order of 1s, the adaptation time is approximately 10s \sim 100s, and according to the experiment in [34], the system time scale when Keller-Segel equation is valid is about 1000s. Therefore, we consider

the long time regime, where the tumbling frequency becomes large (the so-called parabolic scaling). Let

$$(4.1) \quad \frac{T_1}{L/s_0} = \varepsilon, \quad \frac{T_2}{L/s_0} = 1, \quad \text{and} \quad \frac{T}{L/s_0} = \frac{1}{\varepsilon}$$

Then (3.5)-(3.8) become

$$(4.2) \quad \varepsilon \frac{\partial \rho}{\partial t} = -\frac{\partial J_\rho}{\partial x},$$

$$(4.3) \quad \varepsilon \frac{\partial J_\rho}{\partial t} = -v_0^2 \frac{\partial \rho}{\partial x} - \frac{Z}{\varepsilon} J_\rho - \frac{1}{\varepsilon} \frac{\partial Z}{\partial m} (J_q - M J_\rho),$$

$$(4.4) \quad \varepsilon \frac{\partial q}{\partial t} = -\frac{\partial J_q}{\partial x} + F \rho,$$

$$(4.5) \quad \varepsilon \frac{\partial J_q}{\partial t} = -v_0^2 \frac{\partial q}{\partial x} + F J_q + \frac{\partial F}{\partial m} (J_q - M J_\rho) - \frac{Z}{\varepsilon} J_q - \frac{1}{\varepsilon} \frac{\partial Z}{\partial m} M (J_q - M J_\rho).$$

Consider the following asymptotic expansion

$$\begin{aligned} \rho &= \rho^{(0)} + \varepsilon \rho^{(1)} + \cdots, & J_\rho &= J_\rho^{(0)} + \varepsilon J_\rho^{(1)} + \cdots; \\ q &= q^{(0)} + \varepsilon q^{(1)} + \cdots, & J_q &= J_q^{(0)} + \varepsilon J_q^{(1)} + \cdots; \\ M &= M_0 + \varepsilon M_1 + \cdots, & F &= F_0 + \varepsilon F_1 + \cdots, \\ Z &= Z_0 + \varepsilon Z_1 + \cdots. \end{aligned}$$

Matching the $O(1/\varepsilon)$ terms in (4.3) and (4.5) gives

$$Z_0 J_\rho^{(0)} = \frac{\partial Z_0}{\partial m} (M_0 J_\rho^{(0)} - J_q^{(0)}), \quad \text{and} \quad Z_0 J_q^{(0)} = \frac{\partial Z_0}{\partial m} M_0 (M_0 J_\rho^{(0)} - J_q^{(0)}),$$

which implies

$$M_0 J_\rho^{(0)} = J_q^{(0)}, \quad \text{and} \quad J_\rho^{(0)} = J_q^{(0)} = 0.$$

Hence the $O(1)$ term in (4.4) yields

$$F_0 = 0.$$

Equating the $O(\varepsilon)$ terms in (4.2) and (4.4) produces

$$(4.6) \quad \frac{\partial \rho^{(0)}}{\partial t} = -\frac{\partial J_\rho^{(1)}}{\partial x}, \quad \text{and} \quad \frac{\partial q^{(0)}}{\partial t} = -\frac{\partial J_q^{(1)}}{\partial x} + F_1 \rho^{(0)}.$$

Putting together the $O(1)$ terms in (4.3) and (4.5) brings

$$(4.7) \quad -v_0^2 \frac{\partial \rho^{(0)}}{\partial x} - Z_0 J_\rho^{(1)} + \frac{\partial Z_0}{\partial m} (M_0 J_\rho^{(1)} - J_q^{(1)}) = 0$$

$$(4.8) \quad -v_0^2 \frac{\partial q^{(0)}}{\partial x} - Z_0 J_q^{(1)} - \frac{\partial Z_0}{\partial m} M_0 (J_q^{(1)} - M_0 J_\rho^{(1)}) = 0.$$

The above two equations imply

$$\begin{aligned}
 J_\rho^{(1)} &= Z_0^{-1} \left(-v_0^2 \frac{\partial \rho^{(0)}}{\partial x} + \frac{\partial Z_0}{\partial m} (M_0 J_\rho^{(1)} - J_q^{(1)}) \right) \\
 (4.9) \quad &= -Z_0^{-1} v_0^2 \frac{\partial \rho^{(0)}}{\partial x} + Z_0^{-2} \frac{\partial Z_0}{\partial m} \left(-v_0^2 \left(M_0 \frac{\partial \rho^{(0)}}{\partial x} - \frac{\partial q^{(0)}}{\partial x} \right) \right) \\
 &= -Z_0^{-1} v_0^2 \left(1 + (Z_0)^{-1} M_0 \frac{\partial Z_0}{\partial m} \right) \frac{\partial \rho^{(0)}}{\partial x} + Z_0^{-2} v_0^2 \frac{\partial Z_0}{\partial m} \frac{\partial q^{(0)}}{\partial x}
 \end{aligned}$$

By (3.3),

$$q^{(0)} = M_0 \rho^{(0)}.$$

Therefore

$$\begin{aligned}
 J_\rho^{(1)} &= -Z_0^{-1} v_0^2 \frac{\partial \rho^{(0)}}{\partial x} + Z_0^{-2} v_0^2 \frac{\partial Z_0}{\partial m} \left(\frac{\partial q^{(0)}}{\partial x} - M_0 \frac{\partial \rho^{(0)}}{\partial x} \right) \\
 (4.10) \quad &= -Z_0^{-1} v_0^2 \frac{\partial \rho^{(0)}}{\partial x} + Z_0^{-2} v_0^2 \rho^{(0)} \frac{\partial Z_0}{\partial m} \frac{\partial M_0}{\partial x}.
 \end{aligned}$$

Substituting (4.10) into (4.6) gives the K-S equation

$$(4.11) \quad \frac{\partial \rho^{(0)}}{\partial t} = v_0^2 \frac{\partial}{\partial x} \left(Z_0^{-1} \frac{\partial \rho^{(0)}}{\partial x} \right) - v_0^2 \frac{\partial}{\partial x} \left(Z_0^{-2} \frac{\partial Z_0}{\partial m} \frac{\partial M_0}{\partial x} \rho^{(0)} \right).$$

Using (2.6), (3.17) and $M_0 = M_{a_0}$, $Z_0 = z(M_{a_0})$, the K-S equation becomes

$$(4.12) \quad \frac{\partial \rho^{(0)}}{\partial t} = v_0^2 \frac{\partial}{\partial x} \left(Z_0^{-1} \frac{\partial \rho^{(0)}}{\partial x} \right) - \frac{\partial}{\partial x} (\chi_0 \rho^{(0)} \frac{\partial f_0}{\partial x})$$

with $\chi_0 = \frac{v_0^2 \tau^{-1}}{(z_0 + \tau^{-1})^2} N H (1 - a_0)$.

Remark. 1. Instead of (4.1), if we consider

$$\frac{T_1}{L/s_0} = \varepsilon, \quad \frac{T_2}{L/s_0} = \kappa \varepsilon, \quad \text{and} \quad \frac{T}{L/s_0} = \frac{1}{\varepsilon},$$

then the rescaled system becomes

$$\begin{aligned}
 \varepsilon \frac{\partial \rho}{\partial t} &= -\frac{\partial J_\rho}{\partial x}, \\
 \varepsilon \frac{\partial J_\rho}{\partial t} &= -v_0^2 \frac{\partial \rho}{\partial x} - \frac{Z}{\varepsilon} J_\rho - \frac{1}{\varepsilon} \frac{\partial Z}{\partial m} (J_q - M J_\rho), \\
 \varepsilon \frac{\partial q}{\partial t} &= -\frac{\partial J_q}{\partial x} + \frac{1}{\kappa \varepsilon} F \rho, \\
 \varepsilon \frac{\partial J_q}{\partial t} &= -v_0^2 \frac{\partial q}{\partial x} + \frac{1}{\kappa \varepsilon} F J_\rho + \frac{1}{\kappa \varepsilon} \frac{\partial F}{\partial m} (J_q - M J_\rho) - \frac{Z}{\varepsilon} J_q - \frac{1}{\varepsilon} \frac{\partial Z}{\partial m} M (J_q - M J_\rho).
 \end{aligned}$$

When $\kappa \leq O(1/\varepsilon)$, carrying on similar asymptotic expansion will produce the same Keller-Segel limit (4.12) as $\varepsilon \rightarrow 0$. This indicates that when the adaptation time is shorter than $\sqrt{TT_1}$, the Keller-Segel equation is valid for *E. coli* chemotaxis.

2. The velocity scale of individual bacteria is s_0 . The temporal and spacial scales of the system we consider are T and L respectively, therefore the velocity scale of the drift velocity $v_d = J_\rho/\rho$ is L/T . The equation (4.1) implies $v_d/s_0 \sim O(\varepsilon)$,

which means that in the regime where K-S equation is valid, the drift velocity is much smaller than the moving velocity of individual bacteria.

4.2. Connection to the original PBMFT. We shall show that, under certain assumptions, the moment system (3.5)-(3.8) gets to the original PBMFT in [25]. Especially, one of the equations delivers the important physical assumption eqn. (3) in [25].

The macroscopic quantities in the PBMFT in [25] are the cell densities to the right P^+ and to the left P^- , and the total density $\rho_s = P^+ + P^-$ and cell flux $J_s = v_0(P^+ - P^-)$; the average methylation level to the right M^+ and to the left M^- , the methylation difference $\Delta M_s = \frac{1}{2}(M^+ - M^-)$ and the average methylation $M_s = \frac{M^+P^+ + M^-P^-}{P^+ + P^-}$. The model in [25] is

$$(4.13) \quad \frac{\partial \rho_s}{\partial t} = -\frac{\partial J_s}{\partial x},$$

$$(4.14) \quad \frac{\partial J_s}{\partial t} \approx -v_0^2 \frac{\partial \rho_s}{\partial x} - Z J_s - v_0 \frac{\partial Z}{\partial m} \Delta M_s \rho_s,$$

$$(4.15) \quad \frac{\partial M_s}{\partial t} \approx F - \frac{J_s}{\rho_s} \frac{\partial M_s}{\partial x} - \frac{1}{\rho_s} \frac{\partial}{\partial x} (v_0 \Delta M_s \rho_s),$$

together with the physical assumption

$$(4.16) \quad \Delta M_s \approx -\frac{\partial M_s}{\partial x} Z^{-1} v_0,$$

which physically means ΔM_s is approximated by the methylation level difference in the mean methylation field $M_s(x, t)$ over the average run length $v_0 Z^{-1}$, due to the fact that the direction of motion is randomized during each tumble event.

We firstly discuss the connections of (3.1)-(3.2) to the macroscopic quantities in (4.13)-(4.16). By definition, one has

$$(4.17) \quad \rho = P^+ + P^- = \rho_s, \quad J_\rho = v_0(P^+ - P^-) = J_s,$$

$$(4.18) \quad q = M^+P^+ + M^-P^- = M_s \rho_s,$$

$$(4.19) \quad J_q = v_0(M^+P^+ - M^-P^-) = M_s J_s + \frac{v_0 \Delta M_s}{\rho_s} \left(\rho_s^2 - \frac{J_s^2}{v_0^2} \right).$$

Assumption B. Defining the drift velocity $v_d = J_s/\rho_s$, we assume

$$|v_d| \ll v_0.$$

This is a fair assumption since in experiments an individual cell usually travels at a much higher speed than that of chemotaxis.

Applying Assumption B in (4.19) gives

$$(4.20) \quad J_q - M J_\rho \approx v_0 \Delta M_s \rho_s,$$

by which, (3.5), (3.6) and (3.7) become (4.13), (4.14) and (4.15) respectively. In particular, substituting (4.20) into (3.8) produces

$$(4.21) \quad \frac{\partial}{\partial t}(M_s J_s + v_0 \Delta M_s \rho_s) \approx -v_0^2 \frac{\partial}{\partial x}(\rho_s M_s) + \left(F J_s + v_0 \frac{\partial F}{\partial m} \Delta M_s \rho_s \right) - \left(M_s Z J_s + v_0 \frac{\partial(M_s Z)}{\partial m} \Delta M_s \rho_s \right).$$

Using (4.13)-(4.15) yields

$$(4.22) \quad v_0 \rho_s \frac{\partial \Delta M_s}{\partial t} \approx \frac{J_s^2}{\rho_s} \frac{\partial M_s}{\partial x} + \frac{J_s}{\rho_s} \frac{\partial}{\partial x}(v_0 \rho_s \Delta M_s) + v_0 \Delta M_s \frac{\partial J_s}{\partial x} - v_0^2 \rho_s \frac{\partial M_s}{\partial x} + v_0 \rho_s \Delta M_s \left(\frac{\partial F}{\partial M} - Z \right).$$

Assumption B formally implies the terms containing J_s are relatively small in (4.22), and by a quasi-static approximation $\partial \Delta M_s / \partial t \approx 0$, one has the sum of last three terms is approximately zero in (4.22), and thus

$$\Delta M_s \approx v_0 \frac{\partial M_s}{\partial x} \frac{1}{\frac{1}{\rho_s} \frac{\partial J_s}{\partial x} + \frac{\partial F}{\partial m} - Z}.$$

When $Z \gg |\frac{1}{\rho_s} \frac{\partial J_s}{\partial x} + \frac{\partial F}{\partial m}|$, the above equation leads to the important physical assumption (4.16),

$$(4.23) \quad \Delta M \approx -\frac{\partial M}{\partial x} Z^{-1} v_0,$$

which recovers the PBMFT model in [25].

Remark. The model (4.14)–(4.16) is a nonlinear advection-diffusion system. The new moment system (3.5)–(3.8) evolves only linear advection terms and nonlinear reactions, and thus the numerical methods for such a system is well studied [22].

4.3. Numerical comparison to SPECS. To show the validity of the moment system (3.5)–(3.8), numerical comparisons to SPECS will be presented in this subsection. We choose spatial-temporal varying environment to show how the intracellular dynamics affects the *E. coli* behaviors at the population level. Specifically it presents a pattern of traveling attractant concentration wave, in which an interesting reversal of chemotaxis group velocity was revealed in [25].

We consider a circular channel with the travelling wave concentration given by $[L](x, t) = [L]_0 + [L]_A + \sin[\frac{2\pi}{\lambda}(x - ut)]$. The wavelength λ is fixed to be the length of the channel, while the wave velocity u can be tuned. The steady state profiles of all the macroscopic quantities in (3.5)–(3.8) and corresponding SPECS results are compared in Figure 3. The results from SPECS and the moment system are quantitatively consistent. It can be noticed that, when the concentration changes slowly ($u = 0.4 \mu m/s$), the profile of M can catch up with the target value M_{a_0} (defined by $a([L], M_{a_0}) = a_0$), while in the fast-varying environment ($u = 8 \mu m/s$)

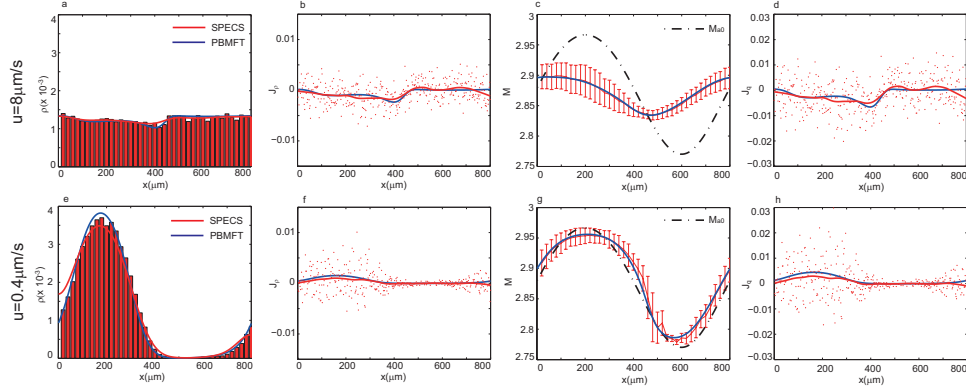


FIGURE 3. Numerical comparison between the new moment system of PBMFT and SPECS. The steady state profiles of ρ : (a, e), J_ρ : (b, f), $M = q/\rho$: (c, g), J_q : (d, h) when the traveling wave speeds are $u = 8\mu m/s$ and $u = 0.4\mu m/s$ respectively. In the subfigures, red lines and dots are from SPECS (red lines in b, d, f, h are the smoothed results of the red dots), while blue lines are from the new moment system of PBMFT. Parameters used here are $[L]_0 = 500\mu M$, $[L]_A = 100\mu M$, $\lambda = 800\mu m$. 20000 cells are simulated in SPECS.

there is a lag in phase between M and M_{a0} . This difference is caused by the slow adaptation rate of cell and it also leads to the difference in the profiles of ρ and even chemotaxis velocity; we refer interested readers to [25] for more detailed discussions and physical explanations.

5. TWO DIMENSIONAL MEAN-FIELD MODEL

In this section, we derive the two-dimensional moment system of PBMFT based on a formal argument using the point-mass assumption in methylation and the minimization principle proposed in [18].

In two dimensions, $\mathbf{v} = v_0(\cos \theta, \sin \theta)$, where v_0 is the velocity magnitude. $P(t, \mathbf{x}, \mathbf{v}, m)$ in (2.7) can be rewritten as $P(t, \mathbf{x}, \theta, m)$. $z(m, [L], \theta, \theta')$ is the tumbling rate from θ' to θ . The tumbling term $Q(P, z)$ in (2.8) becomes

$$(5.1) \quad Q(P, z) = \oint_V z(m, [L], \theta, \theta') P(t, \mathbf{x}, \theta', m) d\theta' - \oint_V z(m, [L], \theta', \theta) d\theta' P(t, \mathbf{x}, \theta, m),$$

where $V = [0, 2\pi)$ and $\oint_V = \frac{1}{2\pi} \int_V$. According to (2.6), $z(m, [L], \theta, \theta')$ is independent of θ and thus we denote it by $z(m, [L])$.

Define

$$(5.2) \quad g(t, \mathbf{x}, \theta) = \int P(t, \mathbf{x}, \theta, m) dm, \quad h(t, \mathbf{x}, \theta) = \int m P(t, \mathbf{x}, \theta, m) dm;$$

$$(5.3) \quad M(t, \mathbf{x}, \theta) = \frac{h(t, \mathbf{x}, \theta)}{g(t, \mathbf{x}, \theta)}, \quad \bar{M}(t, \mathbf{x}) = \frac{\int_V h(t, \mathbf{x}, \theta) d\theta}{\int_V g(t, \mathbf{x}, \theta) d\theta};$$

and the density, density flux, momentum (in m), and momentum flux as follows

$$(5.4) \quad \rho(t, \mathbf{x}) = \int_V g(t, \mathbf{x}, \theta) d\theta, \quad J_\rho(t, \mathbf{x}) = \int_V \mathbf{v} g(t, \mathbf{x}, \theta) d\theta;$$

$$(5.5) \quad q(t, \mathbf{x}) = \int_V h(t, \mathbf{x}, \theta) d\theta, \quad J_q(t, \mathbf{x}) = \int_V \mathbf{v} h(t, \mathbf{x}, \theta) d\theta.$$

We assume

$$(5.6) \quad P(t, \mathbf{x}, \theta, m) = g(t, \mathbf{x}, \theta) \delta(m - M(t, \mathbf{x}, \theta)).$$

This assumption is motivated by (3.19) in one dimension, which could be formally understood as the limit of $k_R \rightarrow +\infty$.

Denote

$$Z = z(\bar{M}, [L]), \quad \frac{\partial Z}{\partial M} = \frac{\partial z}{\partial m}(\bar{M}, [L]), \quad F = f(\bar{M}, [L]), \quad \frac{\partial F}{\partial M} = \frac{\partial f}{\partial m}(\bar{M}, [L]).$$

Integrating (2.7) with respect to m yields

$$(5.7) \quad \partial_t g = -\mathbf{v} \cdot \nabla_{\mathbf{x}} g + \int_V z(M(\theta'), [L]) g(t, \mathbf{x}, \theta') d\theta' - z(M(\theta), [L]) g(t, \mathbf{x}, \theta).$$

Integrating (5.7) with respect to θ gives the equation for density,

$$(5.8) \quad \frac{\partial \rho(t, \mathbf{x})}{\partial t} = -\nabla_{\mathbf{x}} \cdot J_\rho.$$

Multiplying (5.7) by \mathbf{v} and integrating with respect to θ produce

$$(5.9) \quad \begin{aligned} \frac{\partial J_\rho}{\partial t} &= - \int_V \mathbf{v} \otimes \mathbf{v} \nabla_{\mathbf{x}} g d\theta - \int_V \mathbf{v} z(M(\theta), [L]) g(t, \mathbf{x}, \theta) d\theta \\ &\approx - \int_V \mathbf{v} \otimes \mathbf{v} \nabla_{\mathbf{x}} g d\theta - \int_V \mathbf{v} (z(\bar{M}, [L]) + \frac{\partial Z}{\partial m}(M(\theta) - \bar{M})) g(t, \mathbf{x}, \theta) d\theta \\ &= - \int_V \mathbf{v} \otimes \mathbf{v} \nabla_{\mathbf{x}} g d\theta - Z J_\rho - \frac{\partial Z}{\partial m} (J_q - \bar{M} J_\rho), \end{aligned}$$

where we have used the first order Taylor expansion in the second step.

Integrating $m \times (2.7)$ with respect to m brings

$$(5.10) \quad \begin{aligned} \partial_t h &= -\mathbf{v} \cdot \nabla_{\mathbf{x}} h + f(M(\theta), [L]) g(\theta) + \int_V z(M(\theta'), [L]) g(\theta') M(\theta') d\theta' \\ &\quad - z(M(\theta), [L]) g(\theta) M(\theta). \end{aligned}$$

Integrating (5.10) with respect to θ , and using the definition in (5.3) give

$$(5.11) \quad \begin{aligned} \frac{\partial q(\mathbf{x}, t)}{\partial t} &= -\nabla_{\mathbf{x}} \cdot J_q + \int_V f(M(\theta), [L]) g(\mathbf{x}, t, \theta) d\theta \\ &\approx -\nabla_{\mathbf{x}} \cdot J_q + \int_V (f(\bar{M}, [L]) + \frac{\partial f}{\partial m}(M(\theta) - \bar{M})) g(\mathbf{x}, t, \theta) d\theta \\ &= -\nabla_{\mathbf{x}} \cdot J_q + F \rho. \end{aligned}$$

Finally, we integrate $\mathbf{v} \times (5.10)$ with respect to θ ,

$$\begin{aligned}
 (5.12) \quad \frac{\partial J_q}{\partial t} &= - \oint_V \mathbf{v} \otimes \mathbf{v} \cdot \nabla_{\mathbf{x}} h \, d\theta + \oint_V \mathbf{v} (f(M(\theta), [L]) - z(M(\theta), [L])M(\theta)) g(\theta) \, d\theta \\
 &= - \oint_V \mathbf{v} \otimes \mathbf{v} \cdot \nabla_{\mathbf{x}} h \, d\theta + F J_\rho + \frac{\partial F}{\partial m} (J_q - \overline{M} J_\rho) - Z J_q - \frac{\partial Z}{\partial m} \overline{M} (J_q - \overline{M} J_\rho).
 \end{aligned}$$

In order to close the system, especially to find equations for ρ , J , q and J_q , we need to a constitutive relation that represents $\oint_V \mathbf{v} \otimes \mathbf{v} \cdot \nabla_{\mathbf{x}} g \, d\theta$ and $\oint_V \mathbf{v} \otimes \mathbf{v} \cdot \nabla_{\mathbf{x}} h \, d\theta$ by ρ , J , q and J_q . The minimization principle proposed in [18] (mathematically a projection of g and h on the linear space spanned by 1 and \mathbf{v}) gives

$$\begin{aligned}
 (5.13) \quad g(t, \mathbf{x}, \theta) &\approx g_1(t, \mathbf{x}) + g_c(t, \mathbf{x}) \cos \theta + g_s(t, \mathbf{x}) \sin \theta, \\
 h(t, \mathbf{x}, \theta) &\approx h_1(t, \mathbf{x}) + h_c(t, \mathbf{x}) \cos \theta + h_s(t, \mathbf{x}) \sin \theta.
 \end{aligned}$$

Then from (3.1), (3.2),

$$\begin{aligned}
 \rho(t, \mathbf{x}) &\approx \oint_V (g_1 + g_c \cos \theta + g_s \sin \theta) \, d\theta = g_1, \\
 J_\rho(t, \mathbf{x}) &\approx \oint_V \mathbf{v} g(t, \mathbf{x}, \theta) \, d\theta = \frac{v_0}{2} (g_c, g_s)^T, \\
 q(t, \mathbf{x}) &\approx \oint_V (h_1 + h_c \cos \theta + h_s \sin \theta) \, d\theta = h_1 \\
 J_q(t, \mathbf{x}) &\approx \oint_V \mathbf{v} (h_1 + h_c \cos \theta + h_s \sin \theta) \, d\theta = \frac{v_0}{2} (h_c, h_s)^T.
 \end{aligned}$$

Therefore, expressing g_1 , g_c , g_s , M_1 , M_c , M_s by ρ , J_ρ , q , J_q , we find

$$\begin{aligned}
 g_1 &= \rho, & g_c &= \frac{2J_{\rho,x}}{v_0}, & g_s &= \frac{2J_{\rho,y}}{v_0}, \\
 h_1 &= q, & h_c &= \frac{2J_{q,x}}{v_0}, & h_s &= \frac{2J_{q,y}}{v_0},
 \end{aligned}$$

where we denote $\mathbf{x} = (x, y)$ and J_x and J_y are the x and y components of J . Hence,

$$(5.14) \quad \oint_V \mathbf{v} \otimes \mathbf{v} \cdot \nabla g \, d\theta \approx \frac{v_0^2}{2} \nabla g_1 = \frac{v_0^2}{2} \nabla \rho,$$

$$(5.15) \quad \oint_V \mathbf{v} \otimes \mathbf{v} \cdot \nabla h \, d\theta \approx \frac{v_0^2}{2} \nabla h_1 = \frac{v_0^2}{2} \nabla q.$$

Furthermore, since

$$(5.16) \quad \overline{M} = \frac{q}{\rho},$$

we are able to close the system (5.8), (5.9), (5.11), (5.12) using (5.13).

In summary, (5.8), (5.9), (5.11), (5.12) together with (5.14), (5.15) and (5.16) give us a two-dimensional moment system of PBMFT that is similar to (3.5)–(3.8).

6. DISCUSSION AND CONCLUSION

In seek a model at the population level that incorporates intracellular pathway dynamics, we build a new moment system of PBMFT in this paper by using moment closure technique in kinetic theory under the assumption that the methylation level is locally concentrated. The new system is hyperbolic with linear convection terms. Under certain assumptions on the drift velocity, the new system recovers the original model in [25]. Especially the assumption on the methylation difference made in [25] can be understood explicitly in this moment system. We show that when the average run time is much shorter than that of the population dynamics (parabolic scaling), the hydrodynamic limit of the moment system can be described by the Keller-Segal model. We also present numerical evidence to show the quantitative agreement of the moment system with SPECS ([19]).

We remark that the idea of incorporating the underlying signaling dynamics into the classical population level chemotaxis description has appeared in the pioneer works of Othmer *et al* [12, 13, 33]. Here, the internal dynamics follows the physical model proposed in [25], which results in a closure strategy different from [12, 13, 33]. The major differences between the kinetic model in [12, 13, 33] and the one used here are: the methylation rate function is nonlinear (in the methylation level) in [25] while linear in [12, 13, 33]; the tumbling frequency (2.6) follows the results of recent physical studies on chemotaxis ([21, 23]).

Another interesting behavior related to the chemo-sensory system of bacteria is the “volcano effect” observed numerically in [9]. It may be also important to study this phenomena in a more physical way and understand the communications between bacteria using the moment closure technique introduced in this paper, which will be our future study.

APPENDIX

We give a systematic way of obtaining systems with higher order moments by further introducing

(6.1)

$$e(x, t) = \int (m - M)^2 (P^+ + P^-) dm, \quad J_e(x, t) = v_0 \int (m - M)^2 (P^+ - P^-) dm,$$

and finding a system of six variables ρ , q , e , J_ρ , J_q and J_e . The calculations are almost the same as those of deriving (3.5), (3.6), (3.7) and (3.8).

Define M^+ , M^- , M , P_m^\pm , Z , $\frac{\partial Z}{\partial m}$, F and $\frac{\partial F}{\partial m}$ the same as in (3.3), (3.4), and introduce

$$\frac{\partial^2 Z}{\partial m^2} = \frac{\partial^2 z}{\partial m^2} \Big|_{m=M}, \quad \frac{\partial^2 F}{\partial m^2} = \frac{\partial^2 f}{\partial m^2} \Big|_{m=M}.$$

The equation for density ρ is the same as in (3.5). Since we keep more terms in the Taylor approximation for $z(m)$, the equation for the density flux J_ρ becomes

$$\begin{aligned} \frac{\partial J_\rho}{\partial t} &= -v_0^2 \frac{\partial \rho}{\partial x} - v_0 \int z(m)(P^+ - P^-) dm \\ &\approx -v_0^2 \frac{\partial \rho}{\partial x} - v_0 \int \left(z(M) + \frac{\partial z}{\partial m} \Big|_{m=M} (m-M) + \frac{1}{2} \frac{\partial^2 z}{\partial m^2} \Big|_{m=M} (m-M)^2 \right) \\ &\quad \cdot (P^+ - P^-) dm \\ &= -v_0^2 \frac{\partial \rho}{\partial x} - Z J_\rho + \frac{\partial Z}{\partial m} M J_\rho - \frac{\partial Z}{\partial m} J_q - \frac{1}{2} \frac{\partial^2 Z}{\partial m^2} J_e, \end{aligned}$$

Similarly, the equation for q is

$$\frac{\partial q}{\partial t} = -\frac{\partial J_q}{\partial x} + F\rho + \frac{1}{2} \frac{\partial^2 F}{\partial m^2} e.$$

and for J_q is

$$\begin{aligned} \frac{\partial J_q}{\partial t} &= -v_0^2 \frac{\partial q}{\partial x} + F J_\rho + \frac{\partial F}{\partial m} (J_q - M J_\rho) - Z J_q - \frac{\partial Z}{\partial m} M (J_q - M J_\rho) \\ &\quad - \frac{1}{2} \left(-\frac{\partial^2 F}{\partial m^2} + M \frac{\partial^2 Z}{\partial m^2} + 2 \frac{\partial Z}{\partial m} \right) J_e. \end{aligned}$$

We need two additional equations for e and J_e . Since

$$\begin{aligned} e(x, t) &= \int (m-M)^2 (P^+ + P^-) dm = \int m^2 (P^+ + P^-) dm - 2Mq + M^2 \rho \\ &= \int m^2 (P^+ + P^-) dm - Mq, \end{aligned}$$

$$J_e(x, t) = v_0 \int (m-M)^2 (P^+ - P^-) dm = v_0 \int m^2 (P^+ - P^-) dm - 2M J_q + M^2 J_\rho,$$

we can get the equation for e by multiplying both sides of (2.1)+(2.1) by m^2 and integrating with respect to m ,

$$\begin{aligned} \frac{\partial(e + Mq)}{\partial t} &= -\frac{\partial(J_e + 2MJ_q - M^2 J_\rho)}{\partial x} - \int m^2 \frac{\partial(f(a)(P^+ + P^-))}{\partial m} dm \\ &= -\frac{\partial(J_e + 2MJ_q - M^2 J_\rho)}{\partial x} + 2 \int m f(a)(P^+ + P^-) dm \\ &\approx -\frac{\partial(J_e + 2MJ_q - M^2 J_\rho)}{\partial x} + 2 \int \left(MF + \frac{\partial(mf(a))}{\partial m} \Big|_{m=M} (m-M) \right. \\ &\quad \left. + \frac{1}{2} \frac{\partial^2(mf(a))}{\partial m^2} \Big|_{m=M} (m-M)^2 \right) (P^+ + P^-) dm \\ &= -\frac{\partial(J_e + 2MJ_q - M^2 J_\rho)}{\partial x} + 2MF\rho + \left(M \frac{\partial^2 F}{\partial m^2} + 2 \frac{\partial F}{\partial m} \right) e. \end{aligned}$$

The equation for J_e can be obtained by multiplying both sides of (2.1)-(2.1) by $v_0 m^2$ and integrating with respect to m ,

$$\begin{aligned}
& \frac{\partial(J_e + 2MJ_q - M^2J_\rho)}{\partial t} \\
&= -v_0^2 \frac{\partial(e + Mq)}{\partial x} - v_0 \int m^2 \frac{\partial(f(a)(P^+ - P^-))}{\partial m} dm - v_0 \int z(m)m^2(P^+ - P^-) dm \\
&= -v_0^2 \frac{\partial(e + Mq)}{\partial x} + 2v_0 \int mf(a)(P^+ - P^-) dm - v_0 \int z(m)m^2(P^+ - P^-) dm \\
&\approx -v_0^2 \frac{\partial(e + Mq)}{\partial x} + 2v_0 \int \left((mf(a))|_{m=M} + \frac{\partial(mf)}{\partial m}|_{m=M} (m - M) \right. \\
&\quad \left. + \frac{1}{2} \frac{\partial^2(mf)}{\partial m^2}|_{m=M} (m - M)^2 \right) (P^+ - P^-) dm - v_0 \int \left((z(m)m^2)|_{m=M} \right. \\
&\quad \left. + \frac{\partial(z(m)m^2)}{\partial m}|_{m=M} (m - M) + \frac{1}{2} \frac{\partial^2(z(m)m^2)}{\partial m^2}|_{m=M} (m - M)^2 \right) (P^+ - P^-) dm \\
&= -v_0^2 \frac{\partial(e + Mq)}{\partial x} + 2MFJ_\rho + 2\left(M \frac{\partial F}{\partial m} + F\right)(J_q - MJ_\rho) + \left(M \frac{\partial^2 F}{\partial m^2} + 2 \frac{\partial F}{\partial m}\right)J_e \\
&\quad - M^2ZJ_\rho - (2MZ + M^2 \frac{\partial Z}{\partial m})(J_q - MJ_\rho) - \frac{1}{2} \left(\frac{\partial^2 Z}{\partial m^2} M^2 + 4M \frac{\partial Z}{\partial m} + 2Z \right) J_e.
\end{aligned}$$

All these six equations for ρ , J_ρ , q , J_q , e , J_e together give us a closed moment system.

REFERENCES

- [1] J. Adler, *Chemotaxis in bacteria*, Science **153** (1966), 708–716.
- [2] U. Alon, M.G. Surette, N. Barkai, and S. Leibler, *Robustness in bacterial chemotaxis*, Nature **397** (1999), 168–171.
- [3] W. Alt, *Biased random walk models for chemotaxis and related diffusion approximations*, J. Math. Biol. **9** (1980), 147–177.
- [4] H.C. Berg and D.A. Brown, *Chemotaxis in Escherichia coli analysed by three-dimensional tracking*, Nature **239** (1972), 500–504.
- [5] H.C. Berg, *Motile behavior of bacteria*, Physics Today **53** (2000), 24–29.
- [6] P. Biler, L. Corrias, and J. Dolbeault, *Large mass self-similar solutions of the parabolic Keller-Segel model of chemotaxis*, J. Math. Biol. **63** (2011), 1–32.
- [7] A. Blanchet, J.A. Carrillo, and N. Masmoudi, *Infinite time aggregation for the critical patlak-keller-segel model in \mathbb{R}^2* , Comm. Pure Appl. Math. **61** (2008), 1449–1481.
- [8] A. Blanchet, J. Dolbeault, and B. Perthame, *Two-dimensional Keller-Segel model: optimal critical mass and qualitative properties of the solutions*, Electron. J. Differential Equations **44** (2006), 1–32.
- [9] D. Bray, M.D. Levin, and K. Lipkow, *The chemotactic behavior of computer-based surrogate bacteria*, Curr. Biol. **17** (2007), 12–19.
- [10] F.A.C.C. Chalub, P.A. Markowich, B. Perthame, and C. Schmeiser, *Kinetic models for chemotaxis and their drift-diffusion limits*, Monatsh.Math. **142** (2004), 123–141.
- [11] P. Cluzel, M. Surette, and S. Leibler, *An ultrasensitive bacterial motor revealed by monitoring signalling proteins in single cells*, Science **287** (2000), 1652–1655.

- [12] R. Erban and H.G. Othmer, *From individual to collective behavior in bacterial chemotaxis*, SIAM J. Appl. Math. **65** (2004), 361–391.
- [13] ———, *From signal transduction to spatial pattern formation in E. coli: A paradigm for multiscale modeling in biology*, Multiscale Model. Simul. **3** (2005), 362–394.
- [14] F. Filbet, P. Laurencot, and B. Perthame, *Derivation of hyperbolic models for chemosensitive movement*, J. Math. Biol. **50** (2005), 189–207.
- [15] G. L. Hazelbauer, J. J. Falke, and J. S. Parkinson, *Bacterial chemoreceptors: high-performance signaling in networked arrays*, Trends Biochem. Sci. **33** (2008), 9–19.
- [16] G. L. Hazelbauer and S. Harayama, *Sensory transduction in bacterial chemotaxis*, Int. Rev. Cytol. **81** (1983), 33–70.
- [17] T. Hillen and H.G. Othmer, *The diffusion limit of transport equations derived from velocity jump processes*, SIAM J. Appl. Math. **61** (2000), 751–775.
- [18] T. Hillen, *Hyperbolic models for chemosensitive movement*, Math. Models and Methods in Appl. Sci. **12** (2002), 1007–1034.
- [19] L. Jiang, Q. Ouyang, and Y. Tu, *Quantitative modeling of Escherichia coli chemotactic motion in environments varying in space and time*, PLoS Comput. Biol. **6** (2010), e1000735.
- [20] E. Keller and L. Segel, *Model for chemotaxis*, J. Theor. Biol. **30** (1971), 225–234.
- [21] J.E. Keymer, R.G. Endres, M. Skoge, Y. Meir, and N.S. Wingreen, *Chemosensing in escherichia coli: two regimes of two-state receptors*, Proc. Natl. Acad. Sci. U.S.A. **103** (2006), no. 6, 1786.
- [22] R.J. LeVeque, *Numerical methods for conservation laws*, Birkhäuser Verlag, Basel, 1992.
- [23] B.A. Mello and Y. Tu, *Quantitative modeling of sensitivity in bacterial chemotaxis: The role of coupling among different chemoreceptor species*, Proc. Natl. Acad. Sci. **100** (2003), 8223–8228.
- [24] T.S. Shimizu, Y. Tu, and H.C. Berg, *A modular gradient-sensing network for chemotaxis in Escherichia coli revealed by responses to time-varying stimuli*, Mol. Syst. Biol. **6** (2010), 382.
- [25] G. Si, T. Wu, Q. Ouyang, and Y. Tu, *A pathway-based mean-field model for Escherichia coli chemotaxis*, Phys. Rev. Lett. **109** (2012), 048101.
- [26] J.E. Simons and P.A. Milewski, *The volcano effect in bacterial chemotaxis*, Math. Comput. Model. **53** (2011), 1374–1388.
- [27] V. Sourjik and H.C. Berg, *Receptor sensitivity in bacterial chemotaxis*, Proc. Natl. Acad. Sci. **99** (2002), 123–127.
- [28] A. Stevens, *Derivation of chemotaxis-equations as limit dynamics of moderately interacting stochastic many particle systems*, SIAM J. Appl. Math. **61** (2000), 183–212.
- [29] M.J. Tindall, P.K. Maini, S.L. Porter, and J.P. Armitage, *Overview of mathematical approaches used to model bacterial chemotaxis II: bacterial populations*, Bull. Math. Biol. **70** (2008), 1570–1607.
- [30] M.J. Tindall, S.L. Porter, P.K. Maini, G. Gaglia, and J.P. Armitage, *Overview of mathematical approaches used to model bacterial chemotaxis I: the single cell*, Bull. Math. Biol. **70** (2008), 1525–1569.
- [31] Y. Tu, T.S. Shimizu, and H.C. Berg, *Modeling the chemotactic response of escherichia coli to time-varying stimuli*, Proc. Natl. Acad. Sci. U.S.A. **105** (2008), no. 39, 14855.
- [32] G. Wadhams and J. Armitage, *Making sense of it all: bacterial chemotaxis*, Nat. Rev. Mol. Cell Biol. **5** (2004), 1024–1037.
- [33] C. Xue and H.G. Othmer, *Multiscale models of taxis-driven patterning in bacterial populations*, SIAM J. Appl. Math. **70** (2009), 133–167.
- [34] X. Zhu, G. Si, N. Deng, Q. Ouyang, T. Wu, Z. He, L. Jiang, C. Luo, and Y. Tu, *Frequency-dependent Escherichia coli chemotaxis behavior*, Phys. Rev. Lett. **108** (2012), 128101.

CENTER FOR QUANTITATIVE BIOLOGY, PEKING UNIVERSITY, BEIJING, CHINA, 100871, EMAIL:
GWSI@PKU.EDU.CN

INSTITUTE OF NATURAL SCIENCES, DEPARTMENT OF MATHEMATICS AND MOE-LSC, SHANGHAI
JIAO TONG UNIVERSITY, 200240, SHANGHAI, CHINA, EMAIL:TANGMIN@SJTU.EDU.CN

DEPARTMENT OF MATHEMATICS, UNIVERSITY OF CALIFORNIA, SANTA BARBARA, CA 93106,
EMAIL: XUYANG@MATH.UCSB.EDU